

1 Large eddy simulations of surface roughness parameter 2 sensitivity to canopy-structure characteristics

3
4 **K. D. Maurer¹, G. Bohrer¹, W. T. Kenny¹, V. Y. Ivanov²**

5 [1]{Department of Civil, Environmental, & Geodetic Engineering, The Ohio State University,
6 Columbus, OH, USA }

7 [2]{Department of Civil & Environmental Engineering, University of Michigan, Ann Arbor,
8 MI, USA }

9 Correspondence to: G. Bohrer (bohrer.17@osu.edu)

10 11 **Abstract**

12 Surface roughness parameters, namely the roughness length and displacement height, are
13 an integral input used to model surface fluxes. However, most models assume these
14 parameters to be a fixed property of plant functional type and disregard the governing
15 structural heterogeneity and dynamics. In this study, we use large-eddy simulations to
16 explore, *in silico*, the effects of canopy structure characteristics on surface roughness
17 parameters. We performed a virtual experiment to test the sensitivity of resolved surface
18 roughness to four axes of canopy structure: (1) leaf area index, (2) the vertical profile of
19 leaf density, (3) canopy height, and (4) canopy gap fraction. We found roughness
20 parameters to be highly variable, but uncovered positive relationships between
21 displacement height and maximum canopy height, aerodynamic canopy height and
22 maximum canopy height and leaf area index, and eddy-penetration depth and gap
23 fraction. We also found negative relationships between aerodynamic canopy height and
24 gap fraction, and between eddy-penetration depth and maximum canopy height and leaf
25 area index. We generalized our model results into a virtual 'Biometric' parameterization
26 that relates roughness length and displacement height to canopy height, leaf area index
27 and gap fraction. Using a decade of wind and canopy structure observations in a site in
28 Michigan, we tested the effectiveness of our model-driven 'Biometric' parameterization
29 approach in predicting the friction velocity over heterogeneous and disturbed canopies.

1 We compared the accuracy of these predictions with the friction-velocity predictions
2 obtained from the common simple approximation related to canopy height, the values
3 calculated with large eddy simulations of the explicit canopy structure as measured by
4 airborne and ground-based lidar, two other parameterization approaches that utilize
5 varying canopy-structure inputs, and the annual and decadal means of the surface
6 roughness parameters at the site from meteorological observations. We found that the
7 classical representation of constant roughness parameters (in space and time) as a fraction
8 of canopy height performed relatively well. Nonetheless, of the approaches we tested,
9 most of the empirical approaches that incorporate seasonal and inter-annual variation of
10 roughness length and displacement height as a function of the dynamics of canopy
11 structure produced more precise and less biased estimates for friction velocity than
12 models with temporally invariable parameters.

13 **1 Introduction**

14 Our ability to accurately predict mass and energy fluxes from the land surface to the
15 atmosphere at any time scale depends on the accuracy of the surface drag parameterization
16 (Finnigan, 2000;Mahrt, 2010). Over forested environments, vertical mixing of canopy air with
17 the free atmosphere above, which is the process responsible for the exchange of energy, water
18 vapor, and CO₂ between the land surface and the atmosphere, is a function of the turbulent
19 eddies created through interactions between vegetative structure (e.g., trees, tree-stems,
20 leaves) and the wind (Thomas and Foken, 2007a). In many regional models, estimation of
21 surface drag, and thus surface fluxes, is typically dependent upon parameterization of the
22 friction velocity, u_* , based on Monin-Obukhov similarity theory (MOST) (Monin and
23 Obukhov, 1954) using parameters that describe the effects of drag generated by the surface on
24 the shape of the curve describing the vertical distribution of wind speed. These parameters are
25 displacement height, d , and roughness length, z_0 . Though they represent different physical
26 properties of the surface effects on the velocity profile, we will refer to them throughout the
27 manuscript using the combined term 'roughness parameters'. In many land surface, vegetation,
28 ecosystem, and hydrology models, such as the Community Earth System Model (CESM)
29 (Gent et al., 2011), Mapping Evapotranspiration with Internalized Calibration (METRIC)
30 (Allen et al., 2007), and Surface Energy Balance Algorithm for Land (SEBAL) (Bastiaanssen
31 et al., 1998), the surface sensible and latent heat fluxes are functions of the aerodynamic
32 resistance for heat transfer, r_{ah} . r_{ah} is a function of the turbulence at the surface layer, defined

1 through the friction velocity, u_* . In models which cannot directly resolve u_* , r_{ah} is
2 parameterized as a function of d and z_0 . In these models d and z_0 may be derived from
3 different canopy structure characteristics. By the simplest approach, d and z_0 are linear
4 functions of site-level canopy height (h) – typically: $d \approx 0.66h$ (Cowan, 1968) and $z_0 \approx 0.10h$
5 (Tanner and Pelton, 1960). The accuracy of these estimates may be limited, however, by the
6 dynamic nature (space and time) of canopy structural characteristics. First, the canopy is a
7 complex structure that is hard to describe using simple low-variable-number formulations.
8 Second, estimates of the canopy structural characteristics are limited by the typical absence of
9 data about the vertical distribution of leaf area (Massman and Weil, 1999; Shaw and Pereira,
10 1982) and tree-top heights, and the difference between coarse model grid-cell resolution and
11 the finer scale at which canopy structure characteristics vary and affect roughness and
12 momentum and flux transfer.

13 One common approach to incorporate canopy structure in the parameterization of roughness
14 length into models in a more realistic way utilizes satellite imagery products to estimate
15 vegetation structure and relate it to canopy-roughness relationships. For example, the SEBAL
16 model (Moran, 1990) utilizes a function based on the Normalized Difference Vegetation
17 Index (NDVI) while the METRIC model employs Perrier Function (Perrier, 1982). These
18 canopy-roughness relationships have been shown to improve evapotranspiration estimates
19 (Santos et al., 2012), but are specific to sparse or short vegetative environments, such as
20 agricultural systems, and are not typically recommended for forest environments
21 (Bastiaanssen et al., 1998).

22 To incorporate the effects of canopy structure in denser and taller vegetative environments
23 such as forests, empirical functions have been proposed using coarse canopy metrics such as
24 canopy area index (the total, single-sided area of all canopy elements within a $1 \times 1 \text{ m}^2$
25 ground area) (Raupach, 1994), stand density (stems per area), or leaf area index (LAI , the total
26 surface area of leaves found within a $1 \times 1 \text{ m}^2$ vertical column of vegetation) (Nakai et al.,
27 2008a). However, the data required to use these functions are typically not available at most
28 sites and, with the exception of LAI , are not yet obtainable through large-scale satellite remote
29 sensing. In many climate models, surface-layer grid cells are prescribed with biome-specific
30 qualities, i.e., sets of parameters describing constant vegetation structure and flux-driving
31 characteristics for all model cells containing a specific biome or plant functional type (PFT).
32 For example, the Ecosystem Demography model version 2 (ED2, Medvigy et al., 2009)

1 provides twenty different vegetation functional types, seven of which are representative of
2 forested environments, to describe all land surfaces across the globe. Each such vegetation
3 functional type is characterized by fixed, canopy-height driven roughness parameters.
4 Similarly, aerodynamic resistance to surface flux in the advanced hydrological model
5 tRIBS+VEGGIE (Ivanov et al., 2008) is only driven by vegetation height, with is either
6 prescribed, or set as a default per PFT.

7 Roughness parameters have been shown to scale with structural characteristics, such as the
8 influence of area-index (vegetation area per ground area) terms on d and z_0 , through numerical
9 studies (Shaw and Pereira, 1982;Choudhury and Monteith, 1988) and wind-tunnel
10 experiments (Raupach, 1994). Above-canopy meteorology data has shown estimates of
11 roughness parameters to be highly variable both spatially and temporally (Maurer et al.,
12 2013;Harman, 2012;Zhou et al., 2012). As evidence for canopy-roughness relationships has
13 risen, various studies have attempted to generalize small-scale interactions between roughness
14 parameters and canopy structure by deriving d and z_0 from above-canopy meteorological
15 measurements (Braam et al., 2012;Maurer et al., 2013;Raupach et al., 1996;Nakai et al.,
16 2008a), remote-sensing (Schaudt and Dickinson, 2000;Weligepolage et al., 2012), numerical
17 experiments (Grimmond and Oke, 1999;Wouters et al., 2012), and large-eddy simulations
18 (LES) (Aumond et al., 2013;Bohrer et al., 2009;Bou-Zeid et al., 2007;Bou-Zeid et al., 2009).
19 Although the understanding of these small-scale canopy-roughness interactions has grown,
20 accounting for fine-scale canopy structure effects on roughness parameters in larger-scale
21 climate models requires further development.

22 In this study, we use the Regional Atmospheric Modeling System (RAMS)-based Forest
23 Large-Eddy Simulation (RAFLES) (Bohrer et al., 2008;Bohrer et al., 2009) to conduct a
24 virtual experiment to estimate the sensitivity of surface roughness parameters to specific
25 characteristics of fine-scale canopy structure. RAFLES incorporates a prescribed 3-D domain
26 that includes the vegetation leaf density and stem diameters, and dynamically calculates the
27 change to wind velocity as a function of leaf and stem surface drag in each voxel
28 (Chatziefstratiou et al., 2014). The level of detail at which vegetation is represented in
29 RAFLES makes it particularly suitable for conducting this series of virtual experiments that
30 simulate the drag parameters over a simplistic set of virtual canopy structures that vary by
31 structural component, including stand density and patch fraction, canopy height, leaf area
32 index and vertical profile of leaf density. The approach of prescribing drag in LES to resolve

1 site-level roughness was previously tested and shown to provide higher accuracy than the
 2 traditional roughness parameterization (Aumond et al., 2013). Finally, we use 10 years of
 3 direct observations of canopy structure and roughness parameters (Maurer et al., 2013) to
 4 estimate the sensitivity of modelled friction velocity to temporal variation in canopy structure
 5 and its effects on roughness length. We compare these results with other approaches that may
 6 be used to represent canopy structure when modelling roughness parameters.

7 **2 Materials and methods**

8 **2.1 Theory**

9 Monin-Obukhov similarity theory (MOST) describes the relationships between the mean
 10 horizontal wind speed and the friction velocity in the inertial sublayer (Monin and Obukhov,
 11 1954). In brief, MOST describes this relationship using a logarithmic function with
 12 parameters d and z_0 . Further details on the formulation of MOST used in this work are
 13 described in Maurer et al., (2013). The original MOST formulation was expanded to include
 14 the effects of thermal instability and the flow regime in the roughness sub-layer (RSL), as
 15 follows:

$$16 \frac{\kappa \bar{u}_z}{u_*} = \ln\left(\frac{z-d}{z_0}\right) - \psi_m\left(\frac{z-d}{L}\right) + \psi_m\left(\frac{z_0}{L}\right) + I\psi_u\left(\frac{z-d}{L}, \frac{z-d}{z_*-d}\right) \quad (1)$$

17 where \bar{u}_z is the mean horizontal wind speed at height z , above the ground. When the data is
 18 derived from meteorological observations, an over-bar over a variable represents the 30-
 19 minute mean of the 10 Hz time series of that variable. Given the mean eastward and
 20 northward wind velocities, \bar{u} and \bar{v} , \bar{u}_z is rotated toward the wind direction such that:

$$21 \bar{u}_z = \left(\bar{u}^2 + \bar{v}^2\right)^{1/2} \quad (2)$$

22 where κ is the von Kármán constant, ~ 0.4 , z_* is the upper limit of the RSL estimated as $2h$
 23 (Mölder et al., 1999; Raupach et al., 1996), h is the canopy height. I is an indicator function
 24 defined as ($I = 1$ for $z \leq z_*$; or $I = 0$ for $z > z_*$). u_* is the friction velocity defined as:

$$25 u_* = \left(\overline{u'w'^2} + \overline{v'w'^2}\right)^{1/4} \quad (3)$$

1 where each prime term (e.g., w') is the perturbation of the specific variable from its mean
 2 (e.g., $w - \bar{w}$). The atmospheric-stability correction function, $\psi_m(x)$, was described by Paulson
 3 (1970) for unstable atmospheric conditions ($z/L < 0$) as:

$$4 \quad \psi_m(x) = 2 \ln \left[\frac{1 + (1 - 16x)^{1/4}}{2} \right] + \ln \left[\frac{1 + (1 - 16x)^{1/2}}{2} \right] - 2 \tan^{-1} \left[(1 - 16x)^{1/4} \right] + \frac{\pi}{2} \quad (4)$$

5 where x is either $(z - d)/L$ or z_0/L .

6 Current understanding of aerodynamic properties near forest canopies within the roughness
 7 sub-layer (RSL) has led to empirical corrections to the MOST model (Harman and Finnigan,
 8 2007; De Ridder, 2010; Cellier and Brunet, 1992; Garratt, 1980; Mölder et al., 1999; Physick and
 9 Garratt, 1995; Raupach, 1992). These corrections allow us to utilize MOST with
 10 meteorological observation within the RSL, which typically includes the height range where
 11 eddy-covariance measurements of forest flux dynamics are conducted across the globe. The
 12 RSL correction we used, $\psi_u(x_1, x_2)$, was described by De Ridder (2010) as:

$$13 \quad \psi_u(x_1, x_2) = (1 - 16x_1)^{-1/4} \left[\left(1 + \frac{\nu}{\mu \cdot x_2} \right) x_1 \right] \frac{1}{\gamma} \ln \left(1 + \frac{\gamma}{\mu x_2} \right) \exp(-\mu x_2) \quad (5)$$

14 where $x_1 = (z - d)/L$, $x_2 = (z - d)/(z_* - d)$, and ν , μ , and γ are empirical constants
 15 provided by De Ridder (2010) as 0.5, 2.59, and 1.5, respectively. The inclusion of the RSL
 16 correction ($\psi_u \neq 0$) occurs when the calculation is performed within the RSL ($z \leq z_*$, $I = 1$).
 17 Flux data is typically observed within the RSL at one point in space, requiring the
 18 implementation of the RSL correction. When boundary layer conditions are near neutral,
 19 $(z - d)/L$ and z_0/L approach zero, and thus, $\psi_m(x)$ becomes negligible (Eq. 4).

20 Contrary to the classic estimate of z_0 (function of h), Thom (1971) suggested a relationship
 21 between z_0 and $(h - d)$, as opposed to a relationship between z_0 and h alone, where the ratio of
 22 $z_0/(h - d)$ was defined as λ , a dimensionless, stand-specific parameter. This allows z_0 to be
 23 dependent on the spacing of the surface roughness elements and not only their height. For
 24 example, $(h - d)$ will theoretically be smaller for more densely packed surfaces, providing a
 25 smoother surface and smaller roughness length. This relationship can be written as:

$$26 \quad z_0 = \lambda(h - d) \quad (6)$$

1 Nakai et al. (2008b) substituted the aerodynamic height, h_a , for the canopy height, h , into this
2 relationship and rearranged the equation to read:

$$3 \quad h_a = d + \frac{z_0}{\lambda} \quad (7)$$

4 In simulation results, where the detailed 3-D wind field is known, we use Eq. 7 to calculate λ
5 for each simulation using h_a , which can be calculated from the vertical profile of horizontal
6 wind speed and the empirically fitted d and z_0 . It is determined by identifying the height of the
7 inflection point in the vertical wind-speed profile. This height marks the transition between
8 the sub-canopy and above-canopy flow regimes (Thomas and Foken, 2007b).

9 We investigated the eddy penetration depth (δ_e), which is the length scale describing the
10 vertical range from the top of the canopy that is influenced by turbulent mixing from above. It
11 is defined as the distance between h_a and the height where the momentum flux value is 10%
12 of its value at h_a (Nepf et al., 2007).

13 **2.2 Site description**

14 The data used to test the effectivity of our LES-driven, and other modeling approaches
15 originates from a mixed, deciduous forest site at the University of Michigan Biological
16 Station (UMBS) in northern, lower Michigan, USA (45° 33' 35" N, 84° 42' 48" W, elev. 236
17 m above sea level). The forest is dominated (~30% of leaf area index) by early-successional
18 bigtooth aspen (*Populus grandidentata*) and paper birch (*Betula papyrifera*), with a mean age
19 of 85-90 years (Gough et al., 2013). The remaining leaf area is mostly represented by red oak
20 (*Quercus rubra*), red maple (*Acer rubrum*) and white pine (*Pinus strobus*). Mean canopy
21 height is roughly 20-25 m with an average stem density of ≈ 750 stems ha^{-1} (including only
22 trees with DBH > 8 cm). Eddy covariance flux measurements have been ongoing at the site
23 since 1999 and data is available through AmeriFlux (<http://ameriflux.lbl.gov/>), site code: US-
24 UMB. Empirical allometric equations, fitted to measurements in this site (Garrity et al., 2012)
25 are used to determine canopy height from a tree census and measurements of diameter at
26 breast height (DBH). Full censuses were conducted in 2001 and 2010, and partial censuses of
27 DBH for 993 are measured annually. Leaf area index is measured weekly using an optical
28 sensor (LAI2000, Licor Biosciences, Lincoln, NE, USA). Additional details on the calculation
29 of roughness length parameter from wind observations in the site and the determination of
30 canopy structure are described in Maurer et al., (2013). Portable canopy lidar measurements

1 (Hardiman et al., 2013) were used to determine the mean leaf area density profile that was
2 used as the 'natural' leaf area density case. Airborne lidar measurements were conducted by
3 the National Center for Airborne Lidar Mapping (NCALM) in summer 2009. The lidar data
4 and processing for our site are described in Garrity et al., (2012). This dataset was used to
5 determine the mean and variation of canopy top height and gap fraction, and to prescribe the
6 explicit canopy structure in the 'Realistic' LES test case (see section 2.4).

7 **2.3 Large eddy simulations**

8 We used wind fields and heat fluxes from RAFLES simulations results to calculate surface
9 roughness parameters of simplified virtual forests. RAFLES (Bohrer et al., 2009) uses a 3-D
10 heterogeneous canopy domain where leaf and stem areas are prescribed within each voxel.
11 The leaf area density and the instantaneous wind speed within the voxel determine the drag
12 force that is applied to wind flow through that grid cell within each time step. Common to the
13 approach used in most LES, it assumes the leaf area is composed of flat surfaces oriented
14 downstream and neglects higher-order effects of leaf and stem shapes and sub-grid-scale
15 wake generation (shown to be a small effect, Shaw and Patton, 2003). It is combined with
16 radiation attenuation (given the leaf densities in the grid cells above) to determine the sensible
17 and latent heat fluxes emitted from each grid cell. The model uses the finite volume approach
18 for discretization of the simulation domain. It resolves the effects of volume restriction due to
19 the volume of the vegetation (stems, branches) by reducing the aperture areas available for
20 flux exchange between each pair of neighboring grid cells and by reducing the volume that is
21 available for flow within each grid cell according to the volume of the vegetation present
22 (Chatziefstratiou et al., 2014). It resolves sub-grid-scale turbulence using the Deardorff (1978)
23 scheme, and includes a parameterization for sub-grid-scale turbulence dissipation due to leaf
24 drag (Shaw and Patton, 2003).

25 Simulations consisted of three hours of simulation time at a time step of 0.02 s. RAFLES uses
26 a nested time stepping scheme with higher frequency calculations for turbulence and still
27 higher frequency calculations for pressure perturbations. Eight pressure and four turbulence
28 time steps were nested in one model time step. Output data snapshots of all grid cells in the
29 simulation domain were recorded every 2 seconds. The initial 2.5 hours of simulation time
30 were used as a 'spin-up' period to ensure satisfactory turbulent mixing and semi-stability of
31 the vertical profiles of turbulence and potential temperature. The latter half hour of simulation
32 time was used for analysis, consisting of 300 2-sec snapshots.

1 Synthetic virtual domains covered $1.25 \times 1.25 \times 1.4 \text{ km}^3$ (length x width x height) at a
2 horizontal grid spacing of $5 \times 5 \text{ m}^2$, which approximately corresponds to the mean size of
3 individual tree-crowns. Vertical grid spacing was 3 m in the lower sub-domain, from the
4 ground to 100 m above ground level. Above that region, vertical grid spacing was gradually
5 increased by 12% per each subsequent horizontal layer up to a maximal grid spacing of 30 m.
6 The vertical grid spacing then remained constant above that height up to the model top at 1.4
7 km. The model has periodic boundary conditions at the lateral boundaries, no-slip boundary
8 conditions at the bottom boundary and a no-flux top boundary with Rayleigh friction to
9 dampen vertical perturbations at the top 6 model layers (180 m). Initial conditions were
10 horizontally homogeneous and followed a prescribed vertical profile for potential
11 temperature, humidity, and wind speed. The prescribed initial vertical profile of the potential
12 temperature described a well-mixed atmospheric boundary layer and was constant from 50 m
13 to the height of the capping inversion, and increased with height above that level. Latent and
14 sensible heat fluxes were prescribed based on observed mean noontime observations for
15 August 2011 above the canopy at US-UMB. For each column of the horizontal simulation
16 domain, the sum of the fluxes and Bowen ratio were distributed around the prescribed mean
17 as an empirical function of *LAI*. Fluxes were further distributed vertically following a leaf-
18 area dependent empirical exponential profile. More details on the numerical setup of the
19 model and the approach for flux forcing are provided in Bohrer et al. (2009).

20 **2.4 Virtual experiment setup: Sensitivity analysis to quantify the** 21 **effects of specific canopy-structure characteristics on roughness** 22 **parameters**

23 Forest canopies are a complex array of 3-D structures. Many structural characteristics, such as
24 tree height, *LAI*, vertical leaf area density (*LAD*) profile, and gap fraction, among others,
25 affect the airflow inside and above the canopy and, consequently, affect the resulting
26 roughness parameters and aerodynamic properties of the surface that describe such canopy
27 structure. Using synthetic cases representing different aspects of canopy structure, we
28 conducted a virtual experiment to test the sensitivity of roughness parameters to four axes of
29 canopy structure: (1) mean site-level *LAI*, ranging from observed leaf-off conditions ($LAI =$
30 $1.0 \text{ m}^2 \text{ m}^{-2}$) to typical, mid-growing season leaf-on conditions ($LAI > 1.0 \text{ m}^2 \text{ m}^{-2}$); (2) *LAD*
31 (m^2m^{-3}) profile, defined through the vertical bias of the vertical leaf density distribution (See
32 *Appendix Figure 1*); (3) canopy height ranging from 9 to 27 m; and (4) canopy patch-level

1 continuity (gap fraction) ranging from 0 to 50% (see *Appendix Figure 2*). Based on the
 2 available computing resources, we selected twenty combinations of the structural
 3 characteristics listed above. A list of all simulation cases and the canopy-structure
 4 characteristics is presented in Table 1.

5 In the gap fraction cases, canopy gaps were randomly created across the domain ranging from
 6 a single-pixel (25 m², tree-crown scale) to multi-pixel blocks (tens to hundreds m²). A gap
 7 was described by shorter vegetation ($h = 9$ m) and a non-gap (closed canopy) was described
 8 by taller vegetation ($h = 27$ m). It should be noted that we introduced gaps in our horizontally
 9 homogenous canopy using holes of varying sizes and shapes, which was done to minimize the
 10 complexity of the prescribed “heterogeneity” treatment (*Appendix Figure 2*). The resulting
 11 gap-size distribution was arbitrary and may not have been well-representative of an actual,
 12 heterogeneous canopy environment with tree-fall gaps.

13 **2.5 Empirical determination of roughness parameters from simulations** 14 **results**

15 To calculate flux and wind statistics, we first calculated the mean value of each model
 16 variable at each vertical model level over the entire horizontal domain, and over all 300 time
 17 snapshots. We then rotated the horizontal wind coordinates of each vertical level toward the
 18 downstream direction, such that the resulting mean rotated downstream velocity is:

$$19 \quad \langle u_r \rangle_{xyt} = \left(\langle u \rangle_{xyt}^2 + \langle v \rangle_{xyt}^2 \right)^{1/2} \quad (8)$$

20 where $\langle \rangle_{xyt}$ marks an average of the simulation results over all voxels in the x (eastward) y
 21 (northward) and t (temporal, 300 snapshots) dimensions. Although the wind forcing aloft is
 22 eastward, a rotation develops following the Ekman spiral and is further amplified by random
 23 x-y asymmetries in the simulation domain. The rotation for the horizontal coordinate system
 24 of each horizontal layer is necessary to maintain a consistent downstream axis required for
 25 data analysis. After this rotation, we calculated the instantaneous perturbation of the velocity
 26 components from the $\langle \rangle_{xyt}$ average for each voxel in space and time along each horizontal
 27 layer, such that:

$$28 \quad u_r' = u_r - \langle u_r \rangle_{xyt} \quad (9)$$

1 where the prime indicates an instantaneous perturbation from the mean value, in this example
 2 of the u_r (downstream) velocity component. Similar formulation applies to the vertical (w)
 3 and cross-stream (v_r) velocity components. Momentum flux at the down-stream direction was
 4 calculated as:

$$5 \quad \langle u_r' w' \rangle_{xyt} = \left\langle \left(u_r - \langle u_r \rangle_{xyt} \right) \left(w - \langle w \rangle_{xyt} \right) \right\rangle_{xyt} \quad (10)$$

6 See Bohrer et al. (2009) for additional details on the calculation of wind statistics and
 7 momentum fluxes from RAFLES output.

8 We determined the effective aerodynamic canopy height, h_a , by identifying the height of the
 9 inflection point in the vertical wind-speed profile as mentioned previously. To find this point,
 10 we compiled a domain-averaged wind-speed profile using Eq. 8. Then, we determined h_a as
 11 the location where the second derivative of the horizontal wind profile crosses zero. We
 12 approximated this location within the vertical grid resolution using linear interpolation. We
 13 calculated the characteristic domain-averaged u_* for each simulation case by calculating the
 14 horizontal-temporal average u_* for each for each horizontal plane of grid cells within the 3-D
 15 virtual domain and further averaging these vertically over the range from $3.5-4.5h$ (u_* values
 16 are nearly invariable with height in that range). Obukhov length was calculated for each
 17 horizontal plane of grid cells within the 3-D virtual domain as a function of the characteristic
 18 u_* , surface heat flux (prescribed) and the mean potential virtual temperature at each
 19 horizontal plane of grid cells. Next, the vertical profile of horizontal mean wind speed from
 20 all grid layers above $1.5h_a$ and below $4.5h$ (95 m) above ground was fitted to Eq. 1 to
 21 determine d and z_0 using the characteristic friction velocity and the Obukhov length. The
 22 empirical fit was calculated using MATLAB's (version R2013b, The MathWorks, Inc.,
 23 Natick, MA, USA) nonlinear, least-squares fit function: *fit*(). We constrained the solution for
 24 the surface roughness parameters to a physically meaningful range by constraining d to be
 25 between 0 and h_a of the simulated forest and z_0 to be larger than 0.

26 **3 Results**

27 **3.1 Virtual experiment to explore canopy-roughness relationships**

28 We found that d was significantly affected by maximum canopy height (h_{\max}) (3-way
 29 ANOVA, Table 2). We also found that h_a and δ_e were significantly affected by h_{\max} , LAI , and

1 gap fraction (GF) (Table 2). z_0 was not found to be significantly affected by any single aspect
 2 of canopy structure investigated within this study. As suggested by Thom (1971) and Nakai et
 3 al. (2008b) we checked the relationship between z_0 and $(h_a - d)$ and found a significant
 4 relationship ($r^2 = 0.72$, $P < 0.001$). We found a positive relationship between d and h_{\max} (fit
 5 forced through [0,0], Figure 1).

$$6 \quad d = 0.69h_{\max} \quad (11)$$

7 Surprisingly, canopy gaps showed little effect on d . A higher correlation existed between d
 8 and h_{\max} ($r^2 = 0.78$) than between d and mean canopy height ($r^2 = 0.48$) across the gap
 9 fraction sensitivity analysis. There was little change to d with increasing gap fraction, except
 10 for the scenario with 50% gap fraction in the leaf-on simulations, which was significantly
 11 lower. Therefore, the relationship with h_{\max} (which was constant as the number of gaps
 12 increased) was selected instead of mean canopy height (which decreased as the number of
 13 gaps increased). Seasonality (leaf-on vs. leaf-off) also showed surprisingly small differences
 14 in d as height was varied, which had previously been observed at US-UMB (Maurer et al.,
 15 2013).

16 We found positive h_a - h_{\max} and h_a - LAI relationships and a negative h_a -gap fraction (GF)
 17 relationship (Figure 2). We note that a positive h_a - h relationship was previously observed at
 18 US-UMB using 12 years of meteorological data and tree-growth censuses (Maurer et al.,
 19 2013). By utilizing the suite of RAFLES simulations we empirically calculated a single
 20 canopy- h_a relationship as:

$$21 \quad h_{a_b} = h_{\max} + aLAI + bGF + c \quad (12)$$

22 where $a = 0.06$ m, $b = (-)0.69$ m, and $c = (-)0.11$ m.

23 We found a negative δ_e - LAI relationship and positive δ_e - h_{\max} and δ_e - GF relationships (Figure
 24 3). As expected, we found δ_e to be consistently higher during leaf-off periods compared to
 25 leaf-on periods at corresponding heights and gap fractions as wind was better able to penetrate
 26 the sub-canopy. Increased LAI intensified the effect of gap fraction on δ_e as the slope of the
 27 leaf-on fit-line was larger than that of leaf-off periods.

28 Relationships were empirically determined using roughness parameters from each RAFLES
 29 simulation, except for those with ‘unnatural’ vertical LAD profiles (i.e., the ‘Upper’,
 30 ‘Middle’, and ‘Lower’ LAD cases) as no patterns were observed between any roughness

1 parameters and vertical LAD profile. Maximum canopy height was used instead of mean
2 canopy height because maximum canopy height was more tightly correlated with each
3 roughness parameter than mean canopy height. The resulting roughness parameters for each
4 simulation are listed in Table 1.

5 We calculated a 'Biometric' h_{a_b} for the US-UMB site using the relationship we found in the
6 virtual experiment between h_{a_b} and LAI , gap fraction and h_{max} (Eq. 12). To simulate the
7 conditions in our site at US-UMB, we assumed a gap fraction of 5%, which was found by
8 calculating the percent area within the NCALM lidar scan domain with vegetation height less
9 than 2 m. We used the peak growing season site-level mean LAI of 4.2 as measured from
10 2000-2011 (Maurer et al., 2013). A 'Biometric' d was then calculated using Eq. 11. Finally, a
11 'Biometric' z_0 was calculated as:

$$12 \quad z_0 = \lambda(h_{a_b} - d) \quad (13)$$

13 where $\lambda = 0.34$ was determined from Eq. 7 given the set of h_a , d and z_0 values from our
14 simulations through the virtual sensitivity experiment.

15 **3.2 Testing empirical approaches that link roughness parameters to biometric** 16 **measurements**

17 The 'Biometric' approach, derived from our simulation results, provides relationships between
18 easily measurable characteristics of the canopy (i.e., LAI and maximum canopy height) and d
19 and z_0 . In order to evaluate the potential improvement to estimates of u_* using this approach,
20 we compared the accuracy and precision of modeled u_* values using the 'Biometric' approach
21 with those of 5 alternative approaches. We evaluate the resulting friction velocities predicted
22 by each of these six ('Biometric' and 5 alternatives) structure-driven parameterization
23 approaches using 30-min observed values of u_* , canopy height and LAI over multiple years
24 at US-UMB (2000-2011, at 34 m a.g.l). The 5 alternative approaches employed are:

- 25 (1) 'Classical' – fixed $d = 0.66h$ and $z_0 = 0.10h$, where we use $h = 22$ m based on a long-term
26 average over the flux footprint during observation period;
- 27 (2) 'Explicit-LES' – fixed $d = 0.67h$ and $z_0 = 0.094h$ as determined from the simulation results
28 of the 'realistic' LES case;
- 29 (3) 'Yearly Observed' – a purely empirical approach, using the values of d and z_0 calculated

1 from meteorological observations during each growing season at US-UMB from 2000-
 2 2011 (Maurer et al., 2013). In this approach, the values of d and z_0 vary each year
 3 according to observations. d and z_0 were calculated by fitting Eq. 1 to a seasonal set of
 4 half-hourly mean observations of wind speed and friction velocity at twice the canopy
 5 height (46 m a.g.l.) and only during neutral to slightly unstable atmospheric conditions
 6 during daytime. We also tested applicability of shorter-term observations of d and z_0 to
 7 long-term predictions of friction velocity. This test was motivated by the fact that there
 8 are only few sites around the world with more than a decade of data, while short
 9 observation campaigns are more common. We used the observed d and z_0 from each year
 10 to simulate the entire decadal time series of friction velocity. This resulted in 12 different
 11 'Yearly' models. Anecdotally, the most accurate model was associate with observed d and
 12 z_0 from 2008, and the least accurate model with the yearly values from 2005.

13 Numerous past studies have attempted to derive relationships between roughness parameters
 14 and other canopy-structure statistics. We chose two in this study:

15 (4) Raupach (1994) calculated d and z_0 as functions of canopy area index (Λ), drag coefficient
 16 (c_d), and canopy height (h):

$$17 \quad d = \left[1 - \frac{1 - \exp(-\sqrt{2c_d\Lambda})}{\sqrt{2c_d\Lambda}} \right] h \quad (14)$$

18 and

$$19 \quad z_0 = \left[\left(1 - \frac{d}{h} \right) \exp\left(-\frac{\kappa \bar{u}}{u_*} - \eta_h \right) \right] h \quad (15)$$

20 where $c_d = 7.5$, $\eta_h = 0.193$, and $\Lambda = 2nbh/A$, where n is the number of stems in a sample
 21 plot, b is the mean diameter at breast height, h is the mean tree height, and A is the total
 22 ground area within the canopy sampling area. Full plot censuses provided the data to
 23 calculate Λ . These were conducted in 2001 and 2010, and Λ values where linearly
 24 interpolated for the years between the censuses and extrapolated to 2011;

25 (5) Nakai et al. (2008a) calculated d and z_0 as functions of stand density (ρ_s), LAI , and h :

$$26 \quad d = \left[1 - \left(\frac{1 - \exp(-\alpha\rho_s)}{\alpha\rho_s} \right) \left(\frac{1 - \exp(-\beta LAI)}{\beta LAI} \right) \right] h \quad (16)$$

1 and

$$2 \quad z_0 = 0.264 \left(1 - \frac{d}{h} \right) h \quad (17)$$

3 where α and β are 7.24×10^{-4} ha stems⁻¹ and 0.273, respectively, and we used the US-UMB
4 mean stand density of 750 stems ha⁻¹.

5 The values of d and z_0 as determined by each of the parameterization approaches are listed in
6 Table 3. The range for yearly observed mean d values was 18.3-26.0 m and for z_0 0.99-1.99
7 m. The 'Classical' approximation based on h resulted in a significantly lower $d = 14.0$ m
8 (outside the range of the inter-annual variability over 12 years), and a slightly above-range z_0
9 = 2.10 m. The 'Explicit-LES' resulted in a very similar d to the 'Classical' approach. The
10 'Biometric' approach predicted high but within-range d values (24.0-25.0 m) but extreme z_0
11 values (3.64-3.82 m). There was nearly no overlap between the values of z_0 from each of the
12 approaches, indicating poor agreement between approaches for this parameter.

13 **3.3 Improvements to estimates of friction velocity using canopy-** 14 **structure-roughness relationships**

15 Modeled u_* from all six approaches was regressed against observed u_* . The slope and
16 intercept of the fit-line (estimates of accuracy), coefficient of determination (r^2), and root
17 mean square error (estimates of precision) are reported in Table 3. Surprisingly, all
18 parameterization approaches produced similar results, with coefficient of determinations
19 between 0.56 and 0.61, near zero, but significantly negative intercepts between (-)0.052 and (-
20)0.072 (significant margin ± 0.004). The most significant difference between the approaches
21 was in their bias. All approaches (except the 'Yearly Observed' 2008 which was the only one
22 that was not significantly biased) produced a significant positive bias, but the bias varied from
23 near zero to 43% (slope of observed vs. modeled fit-line between 1.01 and 1.431, significant
24 margin ± 0.01). The results of all parameterization approaches are listed in Table 3. We found
25 that the precision of the results obtained by using each of the 12 'Yearly Observed' models
26 over the entire 12-years period to be higher than the combined results of using the observation
27 for each specific year during that year only. The bias of the prediction obtained with the
28 observed d and z_0 , applied to the entire 12-year period varied from no significant bias (using
29 the 2008 parameters) to 1.38 (with the 2005 parameters). The combined (each year with its
30 own parameters) produced an intermediate bias for the friction velocity estimates.

1 The 'Yearly Observed' method is dependent on long term observations of wind, temperature,
2 heat flux and friction velocity, which are rarely available in forest sites. The other methods we
3 tested do not require directly observed roughness parameters. Of these methods, the 'Raupach
4 94' approach had the highest precision and lowest bias (slope = 1.24, $r^2 = 0.604$), the 'Explicit
5 LES approach ranked second and our 'Biometric' approach ranked third, although it
6 performed similarly to the very simple 'Classical' approach. The 'Nakai 08' approach proved
7 to be the least compatible with our site.

8 **4 Discussion**

9 **4.1 Response of roughness parameters to canopy structure change**

10 To date, despite a strong need by the modeling community, there is no single consensus
11 approach that relates roughness length and displacement height to observable properties of
12 canopy structure, such as LAI, height, leaf density and gap fraction. Furthermore,
13 observations in our field site (Maurer et al 2013) and by others (Nakai et al., 2008a) have
14 shown that the roughness parameters in forests are not easily constrained by leaf area or
15 canopy height. Our underlying assumption in setting up this model-based experiment was that
16 the lack of a clear empirical relationship between roughness parameters and canopy structure
17 was due to the complexity of canopy structure. We assumed that different characteristics of
18 the canopy drive different effects on roughness length and displacement height. In real
19 forests, many of the structural characteristics vary in time in different ways, resulting in
20 interacting and sometimes conflicting effects on roughness length and displacement height.
21 We set up a numerical experiment that was designed to separate the effects of different
22 observable characteristics of canopy structure. We also hypothesized that, to some degree, the
23 difficulty in identifying a clear effect of canopy structure on each of the roughness parameters
24 is because roughness length and displacement height values may trade-off, such that similar
25 solutions can be fitted either with low d and high z_0 , or *vice versa* (Nakai et al., 2008a; Nakai
26 et al., 2008b; Maurer et al., 2013).

27 By testing the independent effects of different characteristics of canopy structure through a set
28 of controlled virtual experiments, we indeed found that different roughness parameters were
29 sensitive to different structural characteristics. The aerodynamic canopy height (h_a) and eddy
30 penetration depth (δ_e) were both sensitive to leaf area, canopy height and gap fraction (Figures

1 2,3). In contrast, d was only significantly sensitive to canopy height, while z_0 did not show
2 any significant relationships with any single canopy structure characteristic.

3 We found positive $d-h_{\max}$ and h_a-h_{\max} relationships independent of LAI . A strong correlation
4 had previously been reported between h_a and h (Nakai et al., 2008b;Bohrer et al.,
5 2009;Maurer et al., 2013;Thomas and Foken, 2007b). As canopy height was the only canopy
6 characteristic that varied among the 'canopy height variation' simulations (Table 1.c.), it is
7 reasonable to assume that δ_e would be relatively constant, regardless of canopy height.
8 However, as canopy height increased within our virtual domain, the constant mean site-level
9 LAI was stretched further in the vertical direction. Therefore, the mean leaf density in the
10 upper canopy was smaller for taller canopies resulting in an increased δ_e with canopy height
11 (Figure 3b). In spite of increased δ_e , we also observed a positive $d-h_{\max}$ relationship.
12 Indicating that the increased δ_e only partially compensated for the increase in canopy height,
13 allowing for d to increase linearly with canopy height, but with a slope smaller than 1.

14 We found a linear relationship between h_a and gap fraction. Eddy-penetration depth scaled
15 with gap fraction as well. It was consistently larger during leaf-off periods compared to leaf-
16 on periods, and the presence of higher LAI during the leaf-on periods resulted in a steeper
17 linear slope of the relationship between δ_e and gap fraction (Figure 3c). Intuitively, increased
18 gap fraction should lead to increased δ_e , as more canopy openings allow eddies to penetrate
19 deeper into the canopy. These findings are not surprising, as Shaw et al. (1988) found deeper
20 δ_e at lower LAI . For example, we found that increased LAI and increased gap fraction
21 corresponded to increased horizontal wind speed, momentum flux, and turbulence inside the
22 canopy, below $1h$ (Figures 4, 5, 6). This was likely due to the extension of turbulent eddy
23 penetration deep into canopy gaps, indicated by elevated standard deviation of the vertical
24 velocity, σ_w (a component of the turbulence kinetic energy) in canopy gaps (Figure 6a). Such
25 locations of increased turbulent eddy penetration are less likely to occur in horizontally
26 homogenous canopies (Figure 6b). However, the lack of any relationships between roughness
27 length and gap fraction at all levels below 50% gap (Table 1) was surprising, as Bohrer et al.,
28 (2009) found increases to d , z_0 , and h_a in patchier canopies (more gaps) during leaf-on
29 conditions. The major difference between these two studies was that the scale of the gaps
30 prescribed here – corresponding with 1-2 crown sizes – was typically smaller than those in the
31 Bohrer et al., (2009) experiments.

1 We found no consistent correlations between roughness parameters and the mode of the
2 vertical LAD profile, as the variability in roughness parameters over the range of LAD
3 scenarios was extremely high (Table 1). Although the shape of the vertical profile of wind
4 speed is apparently different between the 'Lower' and the 'Upper' LAD profiles (Figure 7)
5 there was no consistent canopy-wind or canopy-turbulence relationships that could be
6 predicted by the bias of the vertical LAD curve (Figure 7). LAD profiles may change in
7 complex ways across the landscape and over many time scales (seasons, years, decades) due
8 to disturbance or senescence. As our virtual experiment has shown, the effects of the vertical
9 LAD profile are inconsistent with a simple representation of the vertical distribution of LAD
10 using its vertical bias as a single descriptive characteristic. Our results indicate that site-level
11 mean LAI and canopy height are easier to obtain and, in general, provide more reliable
12 characteristics of canopy structure than the vertical profile of LAD.

13 Our simulations did not detect a continuous increase to d or z_0 with LAI , which was
14 inconsistent with several previous wind tunnel or model studies (Choudhury and Monteith,
15 1988; Grimmond and Oke, 1999; Raupach, 1994; Shaw and Pereira, 1982). We also did not
16 find significant relationships with any single property of canopy structure, except between
17 displacement height and canopy height. To a limited degree, this was the result of tradeoffs
18 between the two, as indicated by the fact that h_a , which combines d and z_0 through the slope
19 of their tradeoff curve, λ , was better constrained than d or z_0 alone. However, this tradeoff
20 cannot fully explain the lack of relationship, as we did not find a significant and consistent
21 relationship between z_0 and different canopy structural characteristics even when we assumed
22 a fixed displacement height and fitted only for z_0 (results not shown). Combined, our results
23 indicate that both of our underlying hypotheses were at least partially false, and neither the
24 structural complexity of the canopy, nor the tradeoffs between z_0 and d can fully explain the
25 lack of clear relationship between canopy structure and d and z_0 .

26 The lack of canopy structure effects on z_0 within the virtual sensitivity experiment, and in
27 particular, the lack of consistent seasonal differences between leaf-on and leaf-off periods,
28 may suggest that leaf area is not the primary driver of z_0 . To further understand the drivers of
29 z_0 , we calculated the sensitivity of z_0 to changes in wind speed at a measurement height z
30 above the canopy, $\delta_{z_0 u}$. This can be done by solving Eq. 1 for z_0 assuming neutral conditions,
31 and calculating the sensitivity as the partial derivative of z_0 with respect to \bar{u}_z :

$$\delta_{z_0 u} = \frac{\partial z_0}{\partial \bar{u}_z} = \frac{-\kappa(z-d)}{u_*} \exp\left(\frac{-\kappa \bar{u}_z}{u_*}\right) \quad (17)$$

2 We determine that at low to intermediate mean wind speeds (below 3 m/s), z_0 is extremely
 3 sensitive to variation in \bar{u} , with the derivative being between 5 and 30 (Figure 8). This
 4 indicates that, for an observed variation of 0.1 m/s measured at twice the canopy height the
 5 resulting z_0 will change by 0.5-3 m, which is a full range of the expected z_0 values for a 20 m
 6 tall canopy. At our site in Michigan, 3 m/s was approximately the median wind speed and was
 7 therefore selected to drive the simulations. In reality, variations in half-hourly mean wind
 8 speed at the order of 0.1 m/s can be a result of local variations in the flow field due to
 9 topography, or measurement errors due to instrument placement and calibration. In both reality
 10 and LES, such variations in wind speed at a given measurement point could also be the result
 11 of effects of local modification to the flow field due to specific heterogeneous canopy-surface
 12 structures (which were determined to extend up to $5h$, Raupach and Thom, 1981;Bohrer et al.,
 13 2009), and could also be driven by random large eddies that may affect the 30 minute average
 14 at a specific half hour. We hypothesize that this high sensitivity of z_0 may be inhibiting the
 15 attempts to empirically estimate its relationships with the canopy structural characteristic.

16 **4.2 Integrating canopy-structure characteristics into models**

17 Typically, surface roughness parameterization is used in models to directly or indirectly
 18 predict the friction velocity, which is further used in the surface flux calculations. To test the
 19 performance of different parameterization approaches, we used data from 12 years of wind,
 20 friction velocity, Obukhov length, and canopy structure observations in a forest site in
 21 Michigan. We compared six approaches that differ in whether they do (or do not) incorporate
 22 temporal variation to canopy structure, and in the source of data they require to determine z_0
 23 and d . Surprisingly, but optimistically for the purpose of accurate modeling, all the surface
 24 roughness parameterization approaches we tested resulted in relatively high precision ($r^2 =$
 25 0.58-0.61) in predicting the half-hourly friction velocity over 12 years. This is surprising
 26 because each of the approaches used a different set of values for z_0 and d , which in some
 27 cases, were very far from each other. For example The 'Biometric' and the 'Classical' approach
 28 performed rather similarly, but the 'Biometric' approach z_0 values were about 80% larger than
 29 the 'Classical'. To understand this discrepancy, we calculated the sensitivity of the friction
 30 velocity to variation in z_0 , $\delta_{u^* z_0}$.

$$1 \quad \delta_{u^*z_0} = \frac{\partial u^*}{\partial z_0} = \frac{\bar{\kappa} u^*}{z_0} \left[\ln \left(\frac{(z-d)}{z_0} \right) \right]^2 \quad (18)$$

2 For a case similar to the one we simulated, with a canopy at 22 m and mean wind speed of 3
3 m/s, we found that the friction velocity is not sensitive to changes in roughness length when
4 roughness length is higher than 0.6 m (Figure 8). As a general approximation (following the
5 'Classical' approach), for a forest canopy higher than 10 m, roughness length is expected to be
6 larger than $0.1h = 1$ m. Therefore, while the value of the roughness length parameter is highly
7 sensitive to changes in the half-hourly mean wind speed (Equation 17, Figure 8, Table 1), the
8 resulting friction velocity may not be greatly affected from this variation in the parameter's
9 value.

10 The best performing approach for parameterization of roughness length and displacement
11 height, was obtained using the annually observed values of these parameters. The 'Yearly
12 Observed' model demonstrated ~7% less error than the fixed-in-time 'Classical' canopy-
13 roughness relationships. The combined 'Yearly Observed' approach used the z_0 and d values
14 for each year to predict friction velocity values in the same years. This method performed
15 better than when applying the data observed during a single year to the entire time period.
16 However, the roughness parameters observed during 2011 provided a more accurate and
17 precise model for the entire 12-year time series, than the combined approach. The z_0 and d
18 values observed during 2005 provided the worst model, but still performed better than the
19 'Classical' approach. It is rather intuitive that when observations of z_0 and d exist, they will
20 provide the best approach for modeling of friction velocity (Table 3). Our results indicate that
21 the inter-annual variability of canopy structure that affects roughness length has only a very
22 small effect on the resulting friction velocity. Annual growing-season averages of z_0 and d
23 from any single year can provide a suitable approximation to the decadal time series of
24 roughness length parameter values. However, the low spatial coverage by flux networks over
25 the globe limits the use of this method across large spatial domains.

26 LES with an explicit, prescribed canopy structure based on lidar observations of the canopy at
27 a site can generate a surrogate virtual observations from which to evaluate the roughness
28 parameters. However, these type of simulations are limited in their temporal domain (just a
29 few hours as a representative of an entire decade). They are also dependent on high resolution
30 canopy lidar observations that, to date, are not common. Parameterization approaches which
31 rely on biometric observations, rather than on wind observations, may be the most reliable

1 and broadly available method to estimate long-term roughness parameters. Our ability to
2 estimate canopy structure characteristics such as *LAI*, canopy height, and gap fraction over a
3 broad range of spatial and temporal scales is continuously improving through the use of on-
4 site biometric measurements, and airborne and satellite remote sensing observations (Chen et
5 al., 2002;Jonckheere et al., 2004;Zheng and Moskal, 2009).

6 As an indication for the potential of biometric approaches, the approach suggested by
7 Raupach (1994) performed even better than the combined 'Yearly Observed' approach (Table
8 3). However, this approach relies on stem census observations. While such records are more
9 common than flux sites, there is still no broad global coverage for this type of observation.
10 We tested two biometric approaches that only required more commonly observable canopy
11 characteristics. *LAI*, canopy height, and gap fraction or stand density are required by both the
12 Nakai et al (2008a) approach and the approach derived by the virtual experiments in this
13 study (the 'Biometric' approach) in order to determine z_0 and d . Of the two, our 'Biometric'
14 approach performed better, and also provided slightly better estimates than the 'Classical'
15 approach. Variable success by the three biometric methods may not be surprising – a study by
16 Grimmond and Oke (1999) determined that careful consideration must be given to higher-
17 order structural features of the surface than the ones represented in this study and include in
18 the biometric approaches. Examples of such higher-order structural characteristics include the
19 complexity of organization, and density of roughness elements. Similar reasoning could
20 provide insight towards the poor performance of the method of Nakai et al. (2008a) at US-
21 UMB, which is less dense, taller, and has higher *LAI* than those sites used to parameterize the
22 'Nakai 08' method.

23 The 'Biometric' method presented in this study is essentially a variant of the 'Classical'
24 method, with the major difference being the use of a variable maximum canopy height as
25 opposed to mean canopy height, and adding small perturbations to roughness length based on
26 *LAI* and gap fraction (Eqs. 11-13). The limited success of this method can be attributed to
27 some degree to the limited effect of inter-annual variability of canopy structure. However, a
28 decade of observations in a site represents only a very narrow range of potential canopy
29 structures. Our simulation results suggest that this method could potentially improve the
30 prediction of friction velocity when applied to situations where canopy structural variability is
31 larger, such as after significant disturbance events.

1 5 Conclusions

2 In this study we used an LES, long-term meteorological observations, and remote sensing of
3 the canopy to explore the effects of canopy structure on surface roughness parameters in a
4 forest site. We performed a virtual experiment to test the sensitivity of roughness parameters
5 with respect to four axes of variation in canopy structure: (1) leaf area index, (2) the mode of
6 the vertical profile of LAD, (3) canopy height, and (4) gap fraction. We found consistent
7 relationships between the aerodynamic canopy height and *LAI*, maximum height, and gap
8 fraction and between *d* and maximal canopy height. We found that the predicted values of
9 friction velocity are not sensitive to roughness length. As a result, most of the roughness-
10 based approaches we tested for simulating friction velocity performed similarly well. This is
11 despite having very different approaches for determining the values of z_0 and d , and having
12 large differences in the range of z_0 and d values. This is good news for modelers, because it
13 limits the error from using the current approaches that do not vary in time and do not
14 incorporate canopy structure.

15 Nonetheless, most of the approaches we tested which used annually variable z_0 and d and that
16 incorporated canopy structure provided better approximation for friction velocity than the
17 'Classical', time-invariable method. Many easily obtainable metrics of canopy-structure
18 characteristics are available through a suite of measurements, such as on-site meteorological
19 and biometric observations or satellite-derived site characteristics. Additionally, many
20 ecosystem models and ecosystem modules within earth system models resolve the growth of
21 the forest and accurately predict canopy height and *LAI*. Some models, such as the Ecosystem
22 Demography model (Medvigy et al., 2009) even resolve the distribution of stem sizes. Such
23 demographic models could readily incorporate the approach by Raupach (1994) for a
24 significant improvement in surface roughness parameterization. For other models that resolve,
25 or are forced by observed leaf area and vegetation height, our LES-derived 'Biometric'
26 approach could offer an easy way to dynamically affect the roughness-length
27 parameterization. This could provide an improvement of surface flux modeling, especially
28 when canopy structure variations are large. Due to limited spatial coverage by direct
29 meteorological measurements, remote sensed structure statistics, and stand inventories, we
30 suggest utilizing site- and time-specific biometric measurements of canopy structure to
31 estimate site-level d and z_0 . The effectivity of these model improvements will, of course, be

1 dependent upon the quality, quantity, and resolution of the datasets available at the forest of
2 interest.

3

4 **Acknowledgments**

5 We thank Peter Curtis and Christoph Vogel for running the AmeriFlux US-UMB and US-
6 UMd sites, and for advice in conducting this study. We thank Ashley Matheny for editing the
7 manuscript. We thank Brady Hardiman for the use of LiDAR data provided through an NSF-
8 NCALM graduate seed award. This research was supported by the U.S. Department of
9 Energy's Office of Science, Office of Biological and Environmental Research, Terrestrial
10 Ecosystem Sciences program under Awards No. DE-SC0006708 and DE-SC0007041 and the
11 Ameriflux Management project under Flux Core Site agreement No. 7096915 through
12 Lawrence Berkeley National Laboratory, and additional support by the National Science
13 Foundation grant DEB-0911461. KDM was funded in part by an NSF IGERT Fellowship
14 DGE-0504552 awarded through the UMBS Biosphere-Atmosphere Research Training
15 (BART) program. WTK was funded by NASA Earth and Space Science Graduate Training
16 Fellowship #NNX11AL45H. Simulations for this projects ran at the Ohio Supercomputer
17 under resource allocation project PAS0409-4. Any opinions, findings, and conclusions
18 expressed in this material are those of the authors and do not necessarily reflect the views of
19 the National Science Foundation or the Department of Energy.

20

1 References

- 2 Allen, R., Tasumi, M., Morse, A., Trezza, R., Wright, J., Bastiaanssen, W., Kramber, W.,
3 Lorite, I., and Robison, C.: Satellite-based energy balance for mapping evapotranspiration
4 with internalized calibration (METRIC) - applications, *Journal of Irrigation and Drainage*
5 *Engineering*, 133, 395-406, 10.1061/(ASCE)0733-9437(2007)133:4(395), 2007.
- 6 Aumond, P., Masson, V., Lac, C., Gauvreau, B., Dupont, S., and Berengier, M.: Including the
7 drag effects of canopies: real case large-eddy simulation studies, *Bound. Layer. Meteorol.*,
8 146, 65-80, 10.1007/s10546-012-9758-x, 2013.
- 9 Bastiaanssen, W. G. M., Menenti, M., Feddes, R. A., and Holtslag, A. A. M.: A remote
10 sensing surface energy balance algorithm for land (SEBAL). 1. Formulation, *J. Hydrol.*,
11 212-213, 198-212, 10.1016/S0022-1694(98)00253-4, 1998.
- 12 Bohrer, G., Nathan, R., Katul, G. G., Walko, R. L., and Avissar, R.: Effects of canopy
13 heterogeneity, seed abscission, and inertia on wind-driven dispersal kernels of tree seeds,
14 *J. Ecol.*, 96, 569-580, 10.1111/j.1365-2745.2008.01368.x, 2008.
- 15 Bohrer, G., Katul, G. G., Walko, R. L., and Avissar, R.: Exploring the effects of microscale
16 structural heterogeneity of forest canopies using large-eddy simulations, *Bound. Layer.*
17 *Meteorol.*, 132, 351-382, 10.1007/s10546-009-9404-4, 2009.
- 18 Bou-Zeid, E., Parlange, M. B., and Meneveau, C.: On the parameterization of surface
19 roughness at regional scales, *J. Atmos. Sci.*, 64, 216-227, 10.1175/JAS3826.1, 2007.
- 20 Bou-Zeid, E., Overney, J., Rogers, B. D., and Parlange, M. B.: The effects of building
21 representation and clustering in large-eddy simulations of flows in urban canopies, *Bound.*
22 *Layer. Meteorol.*, 132, 415-436, 10.1007/s10546-009-9410-6, 2009.
- 23 Braam, M., Bosveld, F., and Moene, A.: On Monin-Obukhov scaling in and above the
24 atmospheric surface layer: the complexities of elevated scintillometer measurements,
25 *Bound. Layer. Meteorol.*, 144, 157-177, 10.1007/s10546-012-9716-7, 2012.
- 26 Cellier, P., and Brunet, Y.: Flux-gradient relationships above tall plant canopies, *Agric. For.*
27 *Meteorol.*, 58, 93-117, 10.1016/0168-1923(92)90113-I, 1992.
- 28 Chatziefstratiou, E. K., Velissariou, V., and Bohrer, G.: Resolving the effects of aperture and
29 volume restriction of the flow by semi-porous barriers using large-eddy simulations,
30 *Bound. Layer. Meteorol.*, 152, 329-348, 10.1007/s10546-014-9923-5, 2014.
- 31 Chen, J. M., Pavlic, G., Brown, L., Cihlar, J., Leblanc, S. G., White, H. P., Hall, R. J., Peddle,
32 D. R., King, D. J., Trofymow, J. A., Swift, E., Van der Sanden, J., and Pellikka, P. K. E.:
33 Derivation and validation of Canada-wide coarse-resolution leaf area index maps using
34 high-resolution satellite imagery and ground measurements, *Remote Sens. Environ.*, 80,
35 165-184, 10.1016/S0034-4257(01)00300-5, 2002.
- 36 Choudhury, B. J., and Monteith, J. L.: A four-layer model for the heat budget of
37 homogeneous land surfaces, *Q. J. R. Meteorol. Soc.*, 114, 373-398,
38 10.1002/qj.49711448006, 1988.
- 39 Cowan, I. R.: Mass, heat and momentum exchange between stands of plants and their
40 atmospheric environment, *Q. J. R. Meteorol. Soc.*, 94, 523-544, 10.1002/qj.49709440208,
41 1968.

- 1 De Ridder, K.: Bulk transfer relations for the roughness sublayer, *Bound. Layer. Meteorol.*,
2 134, 257-267, 10.1007/s10546-009-9450-y, 2010.
- 3 Deardorff, J. W.: Closure of 2nd-moment and 3rd-moment rate equations for diffusion in
4 homogeneous turbulence, *Phys. Fluid.*, 21, 525-530, 1978.
- 5 Finnigan, J.: Turbulence in plant canopies, *Annu. Rev. Fluid Mech.*, 32, 519-571,
6 10.1146/annurev.fluid.32.1.519, 2000.
- 7 Garratt, J. R.: Surface influence upon vertical profiles in the atmospheric near-surface layer,
8 *Q. J. R. Meteorol. Soc.*, 106, 803-819, 10.1002/qj.49710645011, 1980.
- 9 Garrity, S. R., Meyer, K., Maurer, K. D., Hardiman, B. S., and Bohrer, G.: Estimating plot-
10 level tree structure in a deciduous forest by combining allometric equations, spatial
11 wavelet analysis and airborne lidar, *Remote Sens. Lett.*, 3, 443-451,
12 10.1080/01431161.2011.618814, 2012.
- 13 Gent, P. R., Danabasoglu, G., Donner, L. J., Holland, M. M., Hunke, E. C., Jayne, S. R.,
14 Lawrence, D. M., Neale, R. B., Rasch, P. J., Vertenstein, M., Worley, P. H., Yang, Z.-L.,
15 and Zhang, M.: The community climate system model version 4, *J. Clim.*, 24, 4973-4991,
16 10.1175/2011jcli4083.1, 2011.
- 17 Gough, C. M., Hardiman, B. S., Nave, L. E., Bohrer, G., Maurer, K. D., Vogel, C. S.,
18 Nadelhoffer, K. J., and Curtis, P. S.: Sustained carbon uptake and storage following
19 moderate disturbance in a Great Lakes forest, *Ecol. Appl.*, 23, 1202-1215, 10.1890/12-
20 1554.1, 2013.
- 21 Grimmond, C. S. B., and Oke, T. R.: Aerodynamic properties of urban areas derived from
22 analysis of surface form, *J. Appl. Meteorol.*, 38, 1262-1292, 10.1175/1520-
23 0450(1999)038<1262:apouad>2.0.co;2, 1999.
- 24 Hardiman, B. S., Bohrer, G., Gough, C. M., and Curtis, P. S.: Canopy structural changes
25 following widespread mortality of canopy dominant trees, *Forests*, 4, 537-552,
26 10.3390/f4030537, 2013.
- 27 Harman, I. N., and Finnigan, J. J.: A simple unified theory for flow in the canopy and
28 roughness sublayer, *Bound. Layer. Meteorol.*, 123, 339-363, 10.1007/s10546-006-9145-6,
29 2007.
- 30 Harman, I. N.: The role of roughness sublayer dynamics within surface exchange schemes,
31 *Bound. Layer. Meteorol.*, 142, 1-20, 10.1007/s10546-011-9651-z, 2012.
- 32 Ivanov, V. Y., Bras, R. L., and Vivoni, E. R.: Vegetation-hydrology dynamics in complex
33 terrain of semiarid areas: II. Energy-water controls of vegetation spatio-temporal
34 dynamics and topographic niches of favorability, *Water Resour. Res.*, 44, W03430,
35 10.1029/2006WR005595, 2008.
- 36 Jonckheere, I., Fleck, S., Nackaerts, K., Muys, B., Coppin, P., Weiss, M., and Baret, F.:
37 Review of methods for in situ leaf area index determination: Part I. Theories, sensors and
38 hemispherical photography, *Agric. For. Meteorol.*, 121, 19-35,
39 10.1016/j.agrformet.2003.08.027, 2004.
- 40 Mahrt, L.: Computing turbulent fluxes near the surface: Needed improvements, *Agric. For.*
41 *Meteorol.*, 150, 501-509, 10.1016/j.agrformet.2010.01.015, 2010.
- 42 Massman, W. J., and Weil, J. C.: An analytical one-dimensional second-order closure model
43 of turbulence statistics and the Lagrangian time scale within and above plant canopies of

- 1 arbitrary structure, *Bound. Layer. Meteorol.*, 91, 81-107, 10.1023/A:1001810204560,
2 1999.
- 3 Maurer, K. D., Hardiman, B. S., Vogel, C. S., and Bohrer, G.: Canopy-structure effects on
4 surface roughness parameters: Observations in a Great Lakes mixed-deciduous forest,
5 *Agric. For. Meteorol.*, 177, 24-34, 10.1016/j.agrformet.2013.04.002, 2013.
- 6 Medvigy, D., Wofsy, S. C., Munger, J. W., Hollinger, D. Y., and Moorcroft, P. R.:
7 Mechanistic scaling of ecosystem function and dynamics in space and time: the
8 Ecosystem Demography model version 2, *J. Geophys. Res.*, 114, G01002,
9 10.1029/2008JG000812, 2009.
- 10 Mölder, M., Grelle, A., Lindroth, A., and Halldin, S.: Flux-profile relationships over a boreal
11 forest — roughness sublayer corrections, *Agric. For. Meteorol.*, 98–99, 645-658,
12 10.1016/S0168-1923(99)00131-8, 1999.
- 13 Monin, A. S., and Obukhov, A. M.: Basic laws of turbulent mixing in the surface layer of the
14 atmosphere, *Tr. Geofiz. Inst. Akad. Nauk SSSR*, 24, 163-187, 1954.
- 15 Moran, M. S.: A satellite-based approach for evaluation of the spatial distribution of
16 evapotranspiration from agricultural lands, PhD, University of Arizona, Tuscon, Arizona,
17 USA., 223 pp., 1990.
- 18 Nakai, T., Sumida, A., Daikoku, K., Matsumoto, K., van der Molen, M. K., Kodama, Y.,
19 Kononov, A. V., Maximov, T. C., Dolman, A. J., Yabuki, H., Hara, T., and Ohta, T.:
20 Parameterisation of aerodynamic roughness over boreal, cool- and warm-temperate
21 forests, *Agric. For. Meteorol.*, 148, 1916-1925, 10.1016/j.agrformet.2008.03.009, 2008a.
- 22 Nakai, T., Sumida, A., Matsumoto, K., Daikoku, K., Iida, S., Park, H., Miyahara, M.,
23 Kodama, Y., Kononov, A. V., Maximov, T. C., Yabuki, H., Hara, T., and Ohta, T.:
24 Aerodynamic scaling for estimating the mean height of dense canopies, *Bound. Layer.
25 Meteorol.*, 128, 423-443, 10.1007/s10546-008-9299-5, 2008b.
- 26 Nepf, H., Ghisalberti, M., White, B., and Murphy, E.: Retention time and dispersion
27 associated with submerged aquatic canopies, *Water Resour. Res.*, 43, W04422,
28 10.1029/2006WR005362, 2007.
- 29 Paulson, C. A.: The mathematical representation of wind speed and temperature profiles in
30 the unstable atmospheric surface layer, *J. Appl. Meteorol.*, 9, 857–861, 10.1175/1520-
31 0450(1970)009<0857:TMROWS>2.0.CO;2, 1970.
- 32 Perrier, A.: Land surface processes: vegetation, in: *Land processes in atmospheric general
33 circulation models*, edited by: Eagleson, P., Cambridge University Press, Cambridge, UK,
34 395-448, 1982.
- 35 Physick, W. L., and Garratt, J. R.: Incorporation of a high-roughness lower boundary into a
36 mesoscale model for studies of dry deposition over complex terrain, *Bound. Layer.
37 Meteorol.*, 74, 55-71, 10.1007/bf00715710, 1995.
- 38 Raupach, M. R., and Thom, A. S.: Turbulence in and above plant canopies, *Annu. Rev. Fluid
39 Mech.*, 13, 97-129, 10.1146/annurev.fl.13.010181.000525, 1981.
- 40 Raupach, M. R.: Drag and drag partition on rough surfaces, *Bound. Layer. Meteorol.*, 60,
41 375-395, 10.1007/bf00155203, 1992.

- 1 Raupach, M. R.: Simplified expressions for vegetation roughness length and zero-plane
2 displacement as functions of canopy height and area index, *Bound. Layer. Meteorol.*, 71,
3 211-216, 10.1007/bf00709229, 1994.
- 4 Raupach, M. R., Finnigan, J. J., and Brunet, Y.: Coherent eddies and turbulence in vegetation
5 canopies: The mixing-layer analogy, *Bound. Layer. Meteorol.*, 78, 351-382,
6 10.1007/BF00120941, 1996.
- 7 Santos, C., Lorite, I. J., Allen, R. G., and Tasumi, M.: Aerodynamic parameterization of the
8 satellite-based energy balance (METRIC) model for ET estimation in rainfed olive
9 orchards of Andalusia, Spain, *Water Resources Management*, 26, 3267-3283,
10 10.1007/s11269-012-0071-8, 2012.
- 11 Schaudt, K. J., and Dickinson, R. E.: An approach to deriving roughness length and zero-
12 plane displacement height from satellite data, prototyped with BOREAS data, *Agric. For.*
13 *Meteorol.*, 104, 143-155, 10.1016/S0168-1923(00)00153-2, 2000.
- 14 Shaw, R. H., and Pereira, A. R.: Aerodynamic roughness of a plant canopy: A numerical
15 experiment, *Agric. Meteorol.*, 26, 51-65, 10.1016/0002-1571(82)90057-7, 1982.
- 16 Shaw, R. H., Denhartog, G., and Neumann, H. H.: Influence of foliar density and thermal-
17 stability on profiles of Reynolds stress and turbulence intensity in a deciduous forest,
18 *Bound. Layer. Meteorol.*, 45, 391-409, 10.1007/BF00124010, 1988.
- 19 Shaw, R. H., and Patton, E. G.: Canopy element influences on resolved- and subgrid-scale
20 energy within a large-eddy simulation, *Agric. For. Meteorol.*, 115, 5-17, 2003.
- 21 Tanner, C. B., and Pelton, W. L.: Potential evapotranspiration estimates by the approximate
22 energy balance method of Penman, *J. Geophys. Res.*, 65, 3391-3413,
23 10.1029/JZ065i010p03391, 1960.
- 24 Thom, A. S.: Momentum absorption by vegetation, *Q. J. R. Meteorol. Soc.*, 97, 414-428,
25 10.1002/qj.49709741404, 1971.
- 26 Thomas, C., and Foken, T.: Flux contribution of coherent structures and its implications for
27 the exchange of energy and matter in a tall spruce canopy, *Bound. Layer. Meteorol.*, 123,
28 317-337, 10.1007/s10546-006-9144-7, 2007a.
- 29 Thomas, C., and Foken, T.: Organised motion in a tall spruce canopy: temporal scales,
30 structure spacing and terrain effects, *Bound. Layer. Meteorol.*, 122, 123-147,
31 10.1007/s10546-006-9087-z, 2007b.
- 32 Weligepolage, K., Gieske, A. S. M., and Su, Z.: Surface roughness analysis of a conifer forest
33 canopy with airborne and terrestrial laser scanning techniques, *Int. J. Appl. Earth Obs.*
34 *Geoinf.*, 14, 192-203, 10.1016/j.jag.2011.08.014, 2012.
- 35 Wouters, H., De Ridder, K., and van Lipzig, N. P. M.: Comprehensive parametrization of
36 surface-layer transfer coefficients for use in atmospheric numerical models, *Bound. Layer.*
37 *Meteorol.*, 145, 539-550, 10.1007/s10546-012-9744-3, 2012.
- 38 Zheng, G., and Moskal, L. M.: Retrieving leaf area index (LAI) using remote sensing:
39 theories, methods and sensors, *Sensors*, 9, 2719-2745, 10.3390/s90402719, 2009.
- 40 Zhou, Y., Sun, X., Ju, W., Wen, X., and Guan, D.: Seasonal, diurnal and wind-direction-
41 dependent variations of the aerodynamic roughness length in two typical forest
42 ecosystems of China, *Terrestrial Atmospheric and Oceanic Sciences*, 23, 181-191,
43 10.3319/tao.2011.10.06.01(a), 2012.

1
2
3
4
5
6

Table 1: Description of simulation cases used for sensitivity analysis of roughness parameters derived from an LES over variable canopy layouts, and the resulting roughness parameters for each simulation case. Canopy structure was varied along four axes: (a) *LAI*, (b) vertical LAD profile, (c) canopy height, (d) gap fraction and (e) realistic.

Experiment	LAI (m ² m ⁻²)	LAD (m ² m ⁻³)	Height (m)	Gap Fraction	<i>d</i> (m)	<i>z</i> ₀ (m)	<i>d</i> / <i>h</i>	<i>z</i> ₀ / <i>h</i>	λ	<i>h</i> _a (m)	δ_e (m)
(a) LAI variation	1.0	Natural	21	0%	14.2	2.6	0.67	0.12	0.38	20.9	13.1
	2.6				13.7	3.1	0.65	0.15	0.41	21.1	11.0
	3.2				16.5	1.3	0.79	0.06	0.27	21.1	10.7
	3.7				7.6	4.0	0.36	0.19	0.29	21.2	9.9
	4.2				16.0	1.2	0.76	0.06	0.24	21.1	10.2
(b) LAD profile variation	4.2	Lower	21	0%	13.6	1.7	0.65	0.08	0.24	20.7	12.6
		Middle			8.8	5.7	0.42	0.27	0.55	19.1	8.2
		Natural			16.0	1.2	0.76	0.06	0.24	21.1	10.2
		Upper			13.8	2.8	0.66	0.14	0.38	21.2	10.2
(c) Canopy height variation	1.0	Natural	9	0%	4.4	0.8	0.49	0.09	0.17	9.3	7.1
			15		3.6	3.5	0.24	0.23	0.31	15.0	10.1
			21		14.2	2.6	0.67	0.12	0.38	20.9	13.1
			27		20.1	2.5	0.74	0.09	0.36	26.9	15.8
	4.2	Natural	9	0%	3.7	2.0	0.41	0.22	0.35	9.4	6.3
			15		8.7	2.5	0.58	0.17	0.38	15.2	7.9
			21		16.0	1.2	0.76	0.06	0.24	21.1	10.2
			27		20.1	2.9	0.75	0.11	0.41	27.1	11.9
(d) Gap fraction variation	1.0	Natural	27	0%	20.1	2.5	0.74	0.09	0.36	26.9	15.8
				10%	19.8	2.2	0.73	0.08	0.31	26.8	17.5
				25%	18.5	3.2	0.69	0.12	0.39	26.8	18.2
				35%	17.9	2.4	0.66	0.09	0.27	26.7	19.2
				50%	18.7	1.8	0.69	0.07	0.23	26.7	20.2
	4.2	Natural	27	0%	20.1	2.9	0.75	0.11	0.41	27.1	11.9
				10%	20.4	2.7	0.76	0.10	0.42	27.0	13.0
				25%	18.7	2.8	0.69	0.11	0.34	27.0	14.4
				35%	19.1	2.4	0.71	0.09	0.30	26.9	15.8
				50%	14.4	4.0	0.53	0.15	0.32	26.9	17.3
(e) Realistic	4.2	Natural	27	5%	18.1	2.5	0.67	0.094	0.43	16.7	10.3

7

1 **Table 2.** Results of a 3-way ANOVA to test any significance maximum canopy height (h_{max}),
2 leaf area index (LAI), and gap fraction (GF) have on displacement height (d), roughness
3 length (z_0), aerodynamic canopy height (h_a), or eddy-penetration depth (δ_e). P -values listed in
4 **bold** font indicate a significant effect.

5

Variable	3-way ANOVA p -value		
	h_{max}	LAI	GF
D	<0.001	0.065	0.370
z_0	0.290	0.227	0.918
h_a	<0.001	<0.001	0.007
δ_e	<0.001	0.001	0.004

6

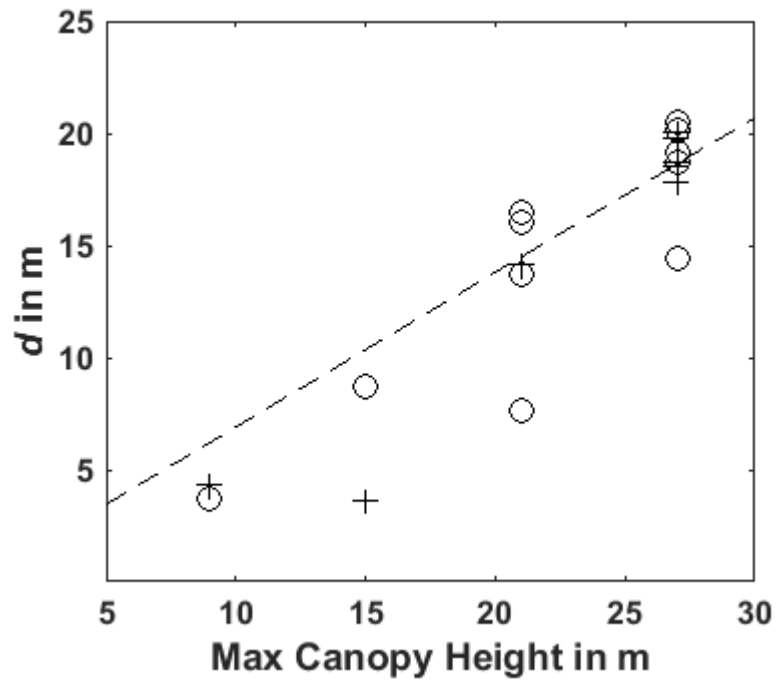
1
2
3
4
5
6
7
8
9

Table 3. 30-min block-averaged friction velocity (u_*) model evaluation against measured u_* for displacement height (d) and roughness length (z_0) calculated from various methods – 'Classical', 'Yearly Observed', 'Biometric', 'Raupach 94', and 'Nakai 08' - at US-UMB spanning the 2000-2011 growing seasons. We show the slope and intercept of the linear fit, which are measures of the accuracy of the models, the coefficient of determination (r^2), which is a measure of precision, and the root mean square error (RMSE) between modeled and observed u_* , which is indicative of both precision and accuracy.

Method		d (m)	z_0 (m)	Slope	Intercept	r^2	RMSE
Classical		14.0	2.10	1.41	-0.05	0.584	0.212
Explicit-LES		18.1	2.54	1.31	-0.06	0.597	0.194
Yearly Obs.	Combined (2000-2011)	23.1 (18.3-26.0)	1.40 (0.99-1.99)	1.11	-0.04	0.564	0.187
	2008 (lowest bias)	26.0	0.99	1.01	-0.06	0.593	0.188
	2011 (highest r^2)	25.0	1.17	1.19	-0.07	0.607	0.179
	2005 (worst)	18.3	1.99	1.38	-0.06	0.588	0.207
Biometric		24.5 (24.0-25.0)	3.74 (3.67-3.82)	1.41	-0.05	0.585	0.212
Raupach 94		17.2 (16.6-17.9)	0.89 (0.88-0.91)	1.24	-0.07	0.604	0.183
Nakai 08		11.5 (11.1-12.0)	2.59 (2.40-2.86)	1.43	-0.05	0.582	0.216

10
11
12

1
2

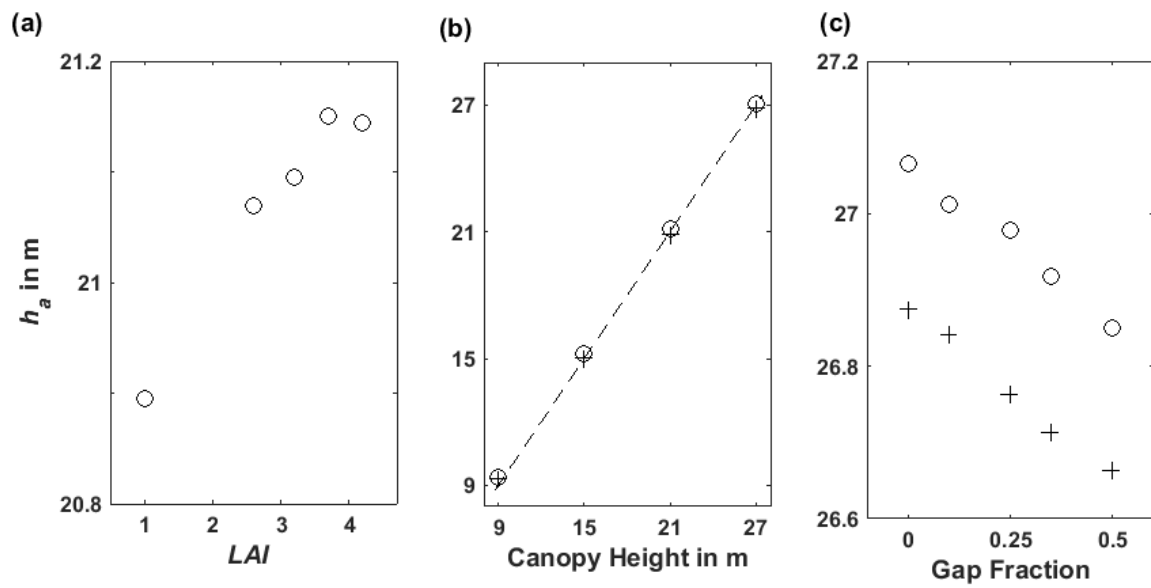


3
4
5
6
7
8

Figure 1. LES domain-averaged d vs. maximum canopy height. Crosses and circles correspond to leaf-off ($LAI = 1.0 \text{ m}^2 \text{ m}^{-2}$) and leaf-on ($LAI > 1.0 \text{ m}^2 \text{ m}^{-2}$) conditions, respectively. Best-fit line (forced through $[0,0]$) shown as dashed line ($d = 0.69h_{\max}$).

1

2

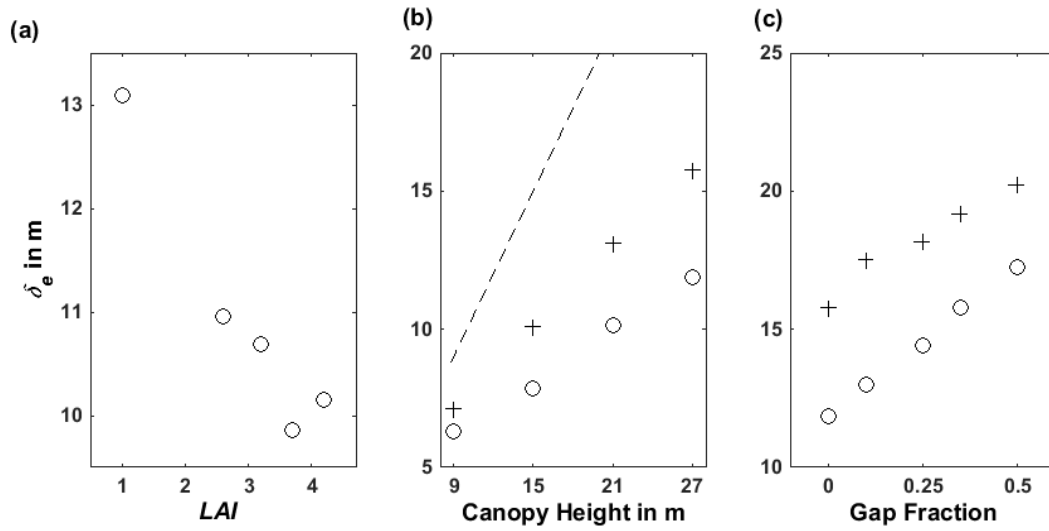


3

4 **Figure 2.** LES domain-averaged aerodynamic canopy height (h_a) vs. (a) leaf area index (LAI),
5 (b) canopy height (h_{max}), and (c) gap fraction (GF). For (b) and (c), crosses and circles
6 correspond to leaf-off and peak- LAI conditions, respectively.

7

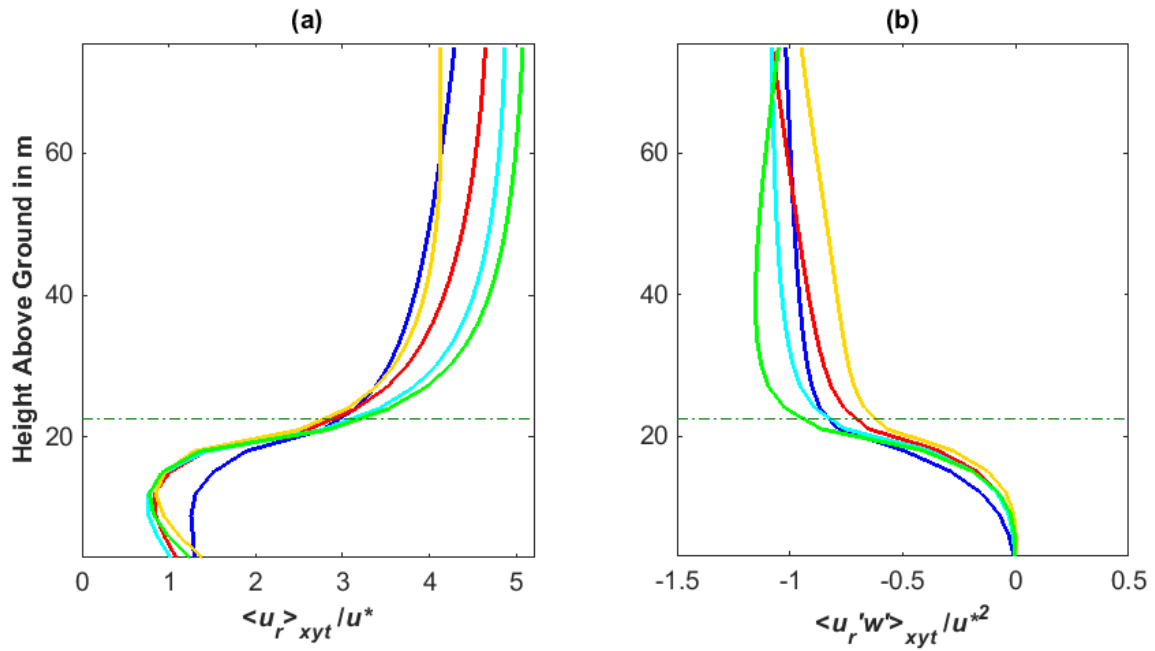
1
2
3



4
5
6
7
8
9

Figure 3. LES domain-averaged eddy-penetration depth (δ_e) vs. (a) leaf area index (LAI), (b) canopy height (h_{max}) and (c) gap fraction (GF). For (b) and (c), crosses and circles correspond to leaf-off and peak- LAI conditions, respectively. The dashed line in panel (b) represents the 1:1 line.

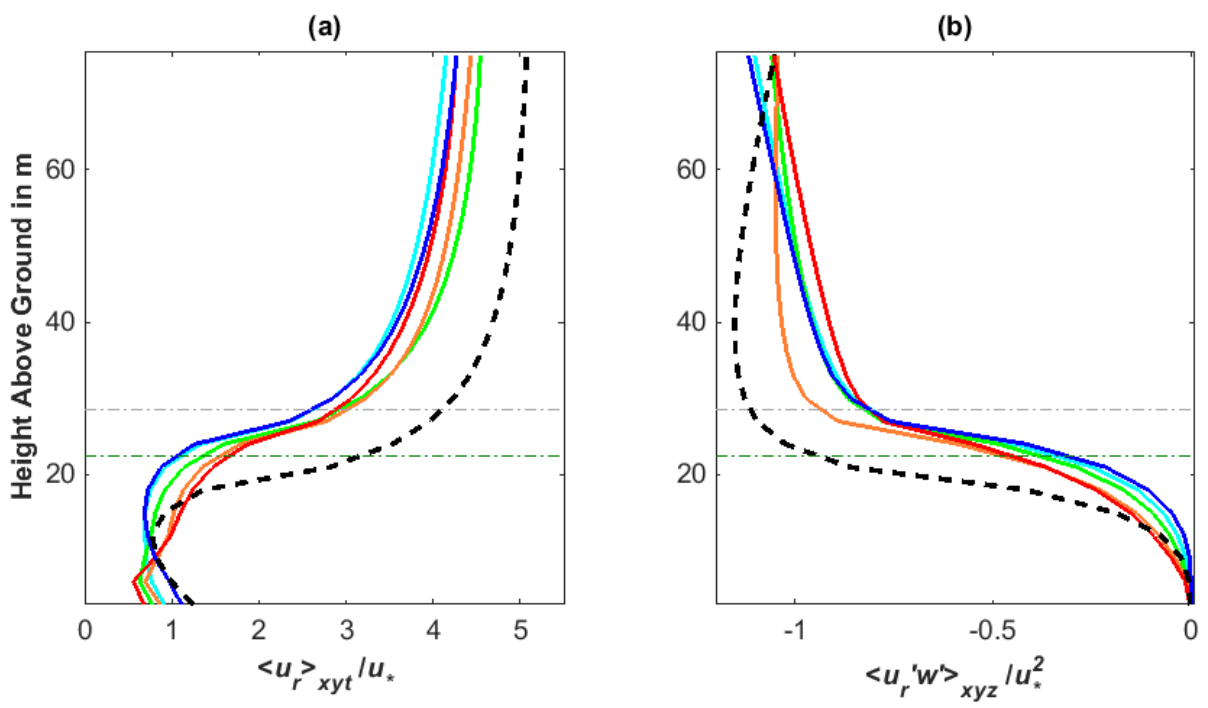
1
2
3



4
5
6
7
8
9

Figure 4. Vertical profiles of (a) Horizontal wind normalized by friction velocity, and (b) momentum flux normalized by the square of friction velocity for $LAI = 1.0 \text{ m}^2 \text{ m}^{-2}$ (blue), $LAI = 2.6 \text{ m}^2 \text{ m}^{-2}$ (cyan), $LAI = 3.2 \text{ m}^2 \text{ m}^{-2}$ (green), $LAI = 3.7 \text{ m}^2 \text{ m}^{-2}$ (orange), and $LAI = 4.2 \text{ m}^2 \text{ m}^{-2}$ (red). Canopy height shown as horizontal dashed green line.

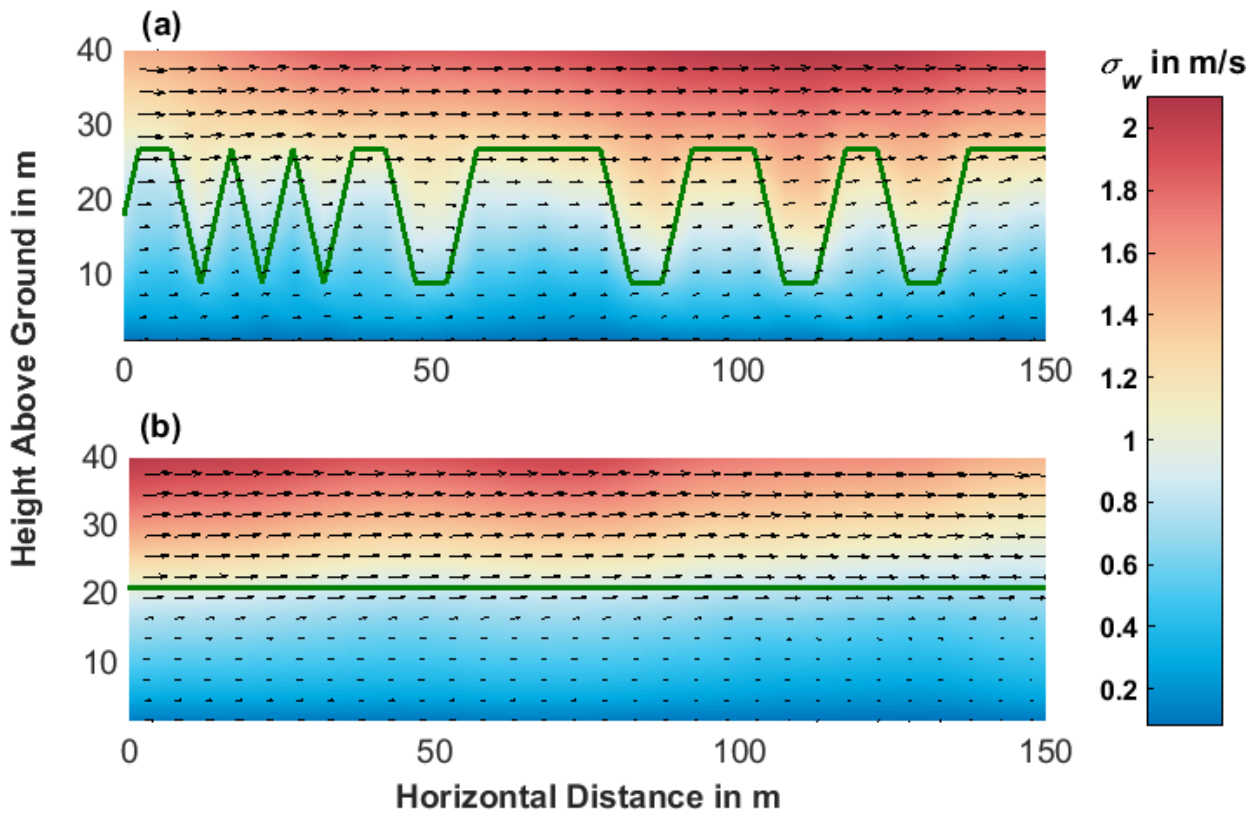
1
2
3



4
5
6
7
8
9
10
11

Figure 5. Vertical profiles of (a) Horizontal wind normalized by friction velocity, and (b) momentum flux normalized by the square of friction velocity in a 27 m tall canopy with gap fractions of 0% (blue), 10% (cyan), 25% (green), 35% (orange), and 50% (red); and in a continuous 21 m tall canopy (dashed back). Canopy height for the tall and short canopies is shown as dashed horizontal gray and green lines, respectively.

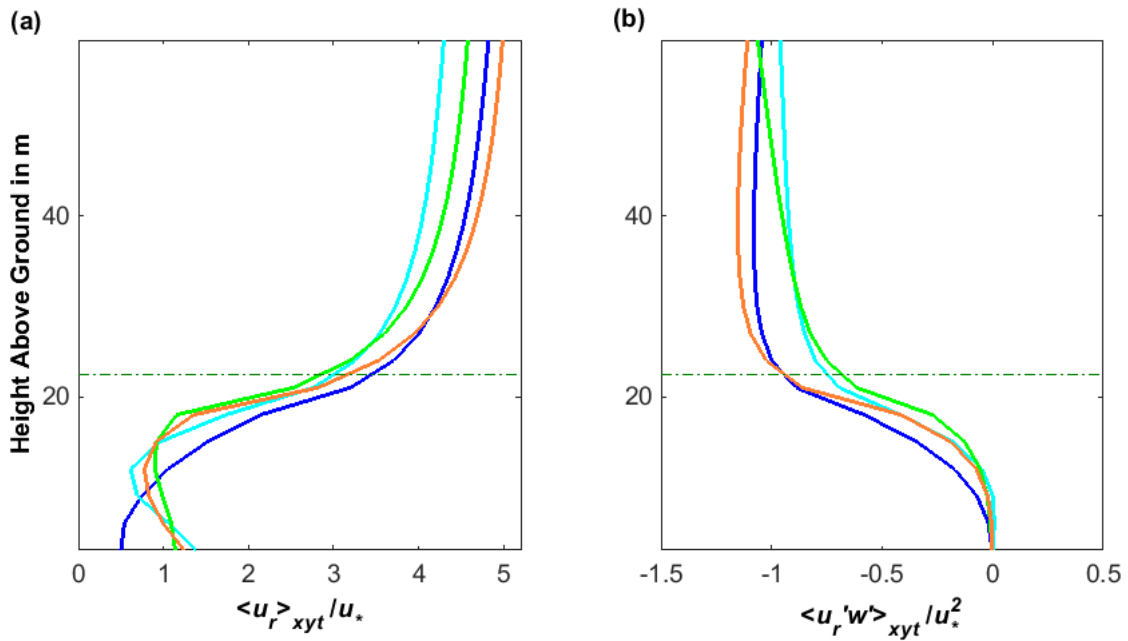
1



2

3 **Figure 6.** Vertical cross-section through the simulation results of (a) a 27 m tall canopy with
4 25% gap fraction and (b) homogeneous 21 m tall canopy. 30-minutes mean wind speed and
5 direction are illustrated using black arrows, the standard deviation of vertical velocity (an
6 indication of turbulence intensity) is plotted using a colormap. Canopy top in each simulation
7 is illustrated by a solid green line.

8



1

2 **Figure 7.** Vertical profiles of (a) Horizontal wind normalized by friction velocity, and (b)
 3 momentum flux normalized by the square of friction velocity for 'Lower' (blue), 'Middle'
 4 ('cyan), 'Upper' (green), and 'Natural' (orange) LAD profiles. Canopy height shown as
 5 dashed horizontal green line.

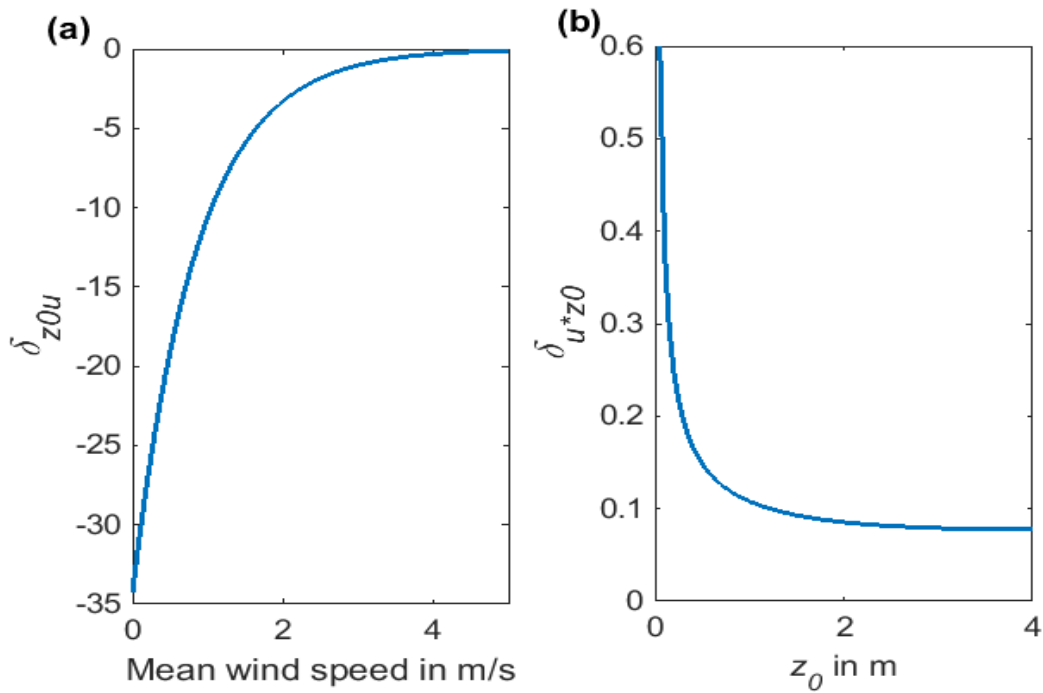
6

7

8

9

10



1

2 **Figure 8.** (a) Sensitivity analysis of z_0 as a function of variation of the mean wind speed
 3 ($\delta_{z_0 u}$). We illustrate it here is a particular range of parameters, choosing a canopy height $h=22$
 4 m (roughly the height we used in the simulation and observation site), displacement height
 5 $d=0.67h$, observation height of $2h$ (the recommended observation height for a flux tower) and
 6 u_* of 0.35 m/s. The results are similar for other canopy heights and u_* values. (b) Sensitivity
 7 of u_* to variation in z_0 ($\delta_{u^* z_0}$). We plotted the response curve over the same parametric range
 8 expected for z_0 values, wind speed at the center range of 3 m/s. u_* is relatively insensitive
 9 ($\delta_{u^* z_0} < 0.15$) for any z_0 above 0.5 m.

10